Intravital imaging of the kidney in a rat model of salt-sensitive hypertension

Bradley T. Endres,[1,2] Ruben M. Sandoval,[4] George J. Rhodes,[4] Silvia B. Campos-Bilderback,[4] Malgorzata M. Kamocka,[4] Christopher McDermott-Roe,[1] Alexander Staruschenko,[1,3] Bruce A. Molitoris,[4] Aron M. Geurts,✉[1,2,3] and Oleg Palygin[1]

[1]Department of Physiology, Medical College of Wisconsin, Milwaukee, Wisconsin;

[2]Department of Human and Molecular Genetics Center, Medical College of Wisconsin, Milwaukee, Wisconsin;

[3]Cardiovascular Center, Medical College of Wisconsin, Milwaukee, Wisconsin; and

[4]Indiana Center for Biological Microscopy, Indiana University School of Medicine, Indianapolis, Indiana

✉Corresponding author.

Address for reprint requests and other correspondence: A. M. Geurts, Dept. of Physiology, Medical College of Wisconsin, 8701 Watertown Plank Rd., Milwaukee, WI 53226 (e-mail: ageurts@mcw.edu).

Abstract

Hypertension is one of the most prevalent diseases worldwide and a major risk factor for renal failure and cardiovascular disease. The role of albuminuria, a common feature of hypertension and robust predictor of cardiorenal disorders, remains incompletely understood. The goal of this study was to investigate the mechanisms leading to albuminuria in the kidney of a rat model of hypertension, the Dahl salt-sensitive (SS) rat. To determine the relative contributions of the glomerulus and proximal tubule (PT) to albuminuria, we applied intravital two-photon-based imaging to investigate the complex renal physiological changes that occur during salt-induced hypertension. Following a high-salt diet, SS rats exhibited elevated blood pressure, increased glomerular sieving of albumin ($GSC_{alb} = 0.0686$), relative permeability to albumin ($+\Delta16\%$), and impaired volume hemodynamics ($-\Delta14\%$). Serum albumin but not serum globulins or creatinine concentration was decreased (-0.54 g/dl), which was concomitant with increased filtration of albumin (3.7 vs. 0.8 g/day normal diet). Pathologically, hypertensive animals had significant tubular damage, as indicated by increased prevalence of granular casts, expansion and necrosis of PT epithelial cells ($+\Delta2.20$ score/image), progressive augmentation of red blood cell velocity ($+\Delta269$ µm/s) and micro vessel diameter ($+\Delta4.3$ µm), and increased vascular injury ($+\Delta0.61$ leakage/image). Therefore, development of salt-induced hypertension can be triggered by fast and progressive pathogenic remodeling of PT epithelia, which can be associated with changes in albumin handling. Collectively, these results indicate that both the

glomerulus and the PT contribute to albuminuria, and dual treatment of glomerular filtration and albumin reabsorption may represent an effective treatment of salt-sensitive hypertension.

Keywords: albuminuria, glomerulus, proximal tubule, chronic kidney disease

---

CHRONIC KIDNEY DISEASE (CKD) is characterized by a progressive loss in kidney function, occurring over the course of months or years, and is estimated to affect more than 25 million adults in the US alone ([1](#), [24](#), [51](#)). The two major causes of CKD are uncontrolled diabetic nephropathy and hypertension, which together contribute to two-thirds of all cases ([41](#)). CKD also predisposes affected individuals to other cardiovascular traits, including dyslipidemia, atherosclerosis, and left ventricular hypertrophy. Canonically, glomerular filtration rate (GFR), which is approximated clinically by measuring serum creatinine levels, is used to define CKD. However, a significant proportion of CKD patients do not exhibit reduced GFR but do exhibit overt albuminuria ([15](#), [26](#), [63](#), [67](#)). Similarly, acute kidney injury patients were shown to exhibit increases in urine albumin before and sometimes in the absence of changes in serum creatinine, suggesting that albumin may serve as a more sensitive biomarker for early diagnosis of renal damage ([6](#), [61](#)). Collectively, these studies suggest that albuminuria represents a more robust predictor of kidney disease and associated cardiorenal pathologies than GFR and raises an interesting question regarding the role of albumin in disease initiation and progression.

The Dahl salt-sensitive (SS) rat is an extensively used and well-established model of salt-induced hypertension and kidney disease that recapitulates many of the clinical features observed in humans with essential hypertension. Upon being fed a high-salt (HS) diet, the SS rat exhibits a rapid and marked increase in mean arterial blood pressure (MAP) and albuminuria ([33](#), [34](#)). Consistent with the human studies described above, albuminuria occurs before any reduction in GFR in SS rats fed a HS diet ([14](#)). The goal of this study was to examine the combined contribution of three renal physiological components, the vasculature, glomeruli, and proximal tubules (PT), to the progression of albuminuria in the SS hypertensive rat. To this end, we applied an intravital two-photon microscopy (ITPM)-based imaging approach ([37](#)) to capture the dynamic nature of renal physiology and investigate changes in renal function that occur during the development of salt-sensitive hypertension. ITPM is able to reveal the complex physiological and pathological changes that occur in the kidney in real-time ([53](#)). This method also allows fluorescent albumin and other molecular markers to be monitored in vivo in the kidney cortex, resulting in the measurement of filtration from the microvasculature and reabsorption at the PT.

Following consumption of a HS diet, SS rats exhibited significant hypertension and albuminuria. Over time, the hypertensive rats began to filter more albumin at the glomerulus. The increased filtration resulted in increased levels of albumin reaching the PT, which normally is reabsorbed and trancytosed back into circulation ([50](#)). In hypertensive rats, we observed a significant reduction in serum albumin as well as changes in albumin reabsorption, which is rapidly increased in response to albumin load and further decay and promotes fast progression of albuminuria primarily because of significant pathological damage that had occurred over time. Concomitantly, changes in the regulation of microvascular blood flow and damage of perivascular capillary bed that can be triggered by PT damage ([11](#), [31](#)) had also occurred after ingestion of a HS diet. Collectively, our data suggest that both the glomerulus and PT cells contribute to albuminuria in the SS hypertensive rats. Furthermore, our results suggest that treatment of salt-sensitive hypertension as well as other forms of CKD would benefit from therapeutic interventions, which preserve, repair, and regenerate the PT.

METHODS

Animals. SS (SS/JrHsdMcwi) rats were maintained initially at the Medical College of Wisconsin. After being weaned, designated rats were sent to the Indiana University School of Medicine, where they were housed until the experiments were performed. Experiments were approved by corresponding Institutional Animal Care and Use Committee. All rats were initially fed a 0.4% sodium chloride AIN-76A diet (Low salt/LS, no. 113755; Dyets). For the experiments, 8- to 10-wk-old male SS rats were either continued to be maintained on a LS diet or switched to a high-salt (HS; 8% NaCl, AIN-76A, no. 100078; Dyets) diet for ≤3 wk. Rats were given water and food ad libitum throughout the study. Serum albumin and globulin collected from anesthetized rats (the whole blood samples were centrifuged at 6,000 rpm/5 min), urine albumin, and creatinine (24 h collection in metabolic cages) were quantified at Marshfield Laboratories (a division of the Marshfield Clinic, Milwaukee, WI). Blood pressure studies were performed using implanted telemetry devices (DSI).

Surgical procedures, two-photon microscopy, and image analysis. In vivo phenotypic characterization of the experimental SS rats using multiphoton microscopy was performed at the Indiana University School of Medicine. All surgical, imaging, and image analysis procedures were performed as described previously (48, 50). Imaging was conducted using an Olympus FV1000 microscope adapted for ITPM with high-sensitivity gallium arsenide nondescanned 12-bit detectors with animal preparations, as described previously (44). Animals were anesthetized with pentobarbital sodium (50 mg/ml). A jugular venous line was used to introduce fluorescent albumin and high-molecular weight dextran. Animal body temperature and heart rate and blood pressure (90 mmHg average) were measured using LabChart 6 (AD Instruments, Colorado Springs, CO).

Quantitation of GSC and PT cell albumin uptake. Glomerular sieving coefficients for albumin (GSCs) were determined using our previously published method (50). Briefly, z-stack images of the glomerulus before TR-albumin infusion were collected to quantify the background fluorescent levels of the Bowman's space and glomerular capillaries. These values were subtracted from the same region after fluorescent albumin infusion. PT reabsorption was calculated using three-dimensional reconstruction of intravital images of PT segments taken between 10 and 30 min postinfusion of TR-albumin. To calculate the absorption of albumin, fluorescent intensity was measured in individual PT using color deconvolution filter with manual selection of the region of interest. Obtained values were denoted as arbitrary fluorescence units (AU). Data distribution was fitted in a Nonlinear Curve Fit module (Origin Pro 9.0; OriginLab, Northampton, MA) using exponential linear function with Levenberg-Marquardt iteration algorithm. Quantification of intensity values was performed using Metamorph (Molecular Devices) or Fiji (ImageJ 1.47v; National Institutes of Health). Using the data generated from our studies, filtered albumin was calculated by using serum albumin and GSC for albumin and mean values for GFR reported previously (14) by the following equation: GFR × 1,440 min × serum albumin (mg/ml) × GSC (65).

Quantitation of vascular extravasation in the kidney cortex. Vascular extravasation was observed using intravital microscopy after intravenous injection of high-molecular weight, 150-kDa FITC-labeled dextran. After 5 min postinjection, at least eight to 10 microphotographs from randomly selected areas were collected for each experimental animal. Indexed color images [LUT: Rainbow RGB (Fiji)] were scored on a scale from 0 to 3, where 0 was no leakage of 150-kDa FITC-Dextran into the interstitial space, 1 was some leakage into a portion of the image (<50%), 2 was all of the interstitial space that had 150-kDa Dextran leaking into it throughout the field, and 3 was the permeability being so high that the intensity within the

interstitial space closely matched the plasma intensity.

In vitro glomerular albumin permeability. Rats were infused with FITC-labeled albumin, and kidneys were harvested and glomeruli isolated by gradual sieving, as described previously (23). Glomeruli were placed in 5% BSA/RPMI solution with high-molecular (150 kDa) TRITC-labeled dextran (TdB Consultancy, Uppsala, Sweden). Fluorescence intensities, detected with the FITC and TRITC filters, were monitored by the confocal laser-scanning microscope system Leica TCS SP8 (Leica Microsystems, Buffalo Grove, IL) and represent inner and outer glomerular space, respectively. Z-stacks of 26 consecutive focal planes (73.83 μm) were collected every 2 min, which allowed reconstructing of fluorescence within glomerular capillaries (FITC) and glomeruli volume (TRITC) using the Fiji image-processing package (ImageJ 1.47v) and OriginPro 9.0 (OriginLab). Water dilution of inner glomerular fluorescence and volume changes created by the oncotic pressure were induced by switching the surrounding medium from 5 to 1% BSA, which was monitored by 3D imaging throughout the experiment. For glomerular volume reconstitution, the TRITC signal was inverted and each focal plane processed by the Analyze Particles module (Fiji). Final glomerular volume was calculated by integration of obtained focal plane areas using OriginPro software. Total glomerular FITC fluorescence within a z-stack was calculated as a sum of the slices' intensities (22). The volume and fluorescence changes represent the alterations in the glomeruli permeability to protein in vivo. Corresponding changes in albumin reflection coefficients (σ_{alb}) were determined by calculating the ratio of observed changes in glomeruli volume (TRITC signal) or percent change in fluorescence (FITC signal) to expected changes in volume or fluorescence, respectively, that are equal to the percent change in the albumin concentration in the bath. Changes in relative albumin permeability, P_{alb}, were calculated as $\Delta(1-\sigma_{alb})$, similar to protocols described earlier (20, 47, 52).

Renal damage scoring. Three-dimensional ×20 images were taken using the two-photon microscope after infusion of Hoechst, TR-albumin, and 150-kDa FITC dextran. Damage severity was scored on a scale of 0–3, where 0 meant there was no damage present and 3 meant there were multiple apoptotic and sclerotic lesions present and significant tubular dilation due to the presence of cast material. All images were scored by two blinded subjects, and the results were averaged.

Histochemistry. For kidney damage analysis, the tissue was stained with Masson's trichrome. Briefly, formalin-fixed kidney sections were cut into 4-μm slices, dried, and deparaffinized for subsequent streptavidin-biotin immunohistochemistry. After deparaffinization, the slides were treated with a citrate buffer (pH 6) for a total of 35 min. The slides were blocked with a peroxidase block (DAKO, Carpinteria, CA), Avidin Block (Vector Laboratories, Burlingame, CA), Biotin Block (Vector), and serum-free Protein Block (DAKO).

Statistical analysis. Statistical analysis was performed using OriginPro 9.0 (OriginLab). Data were expressed as means ± SE and assessed for significance using a one-way ANOVA with a Bonferroni post hoc test or another appropriate statistical test as indicated in the text. A probability value of $P < 0.05$ was considered significant.

RESULTS

Development of albuminuria in SS rats. The effects of HS diet consumption on blood pressure and urinary albumin excretion in SS rats have been demonstrated previously (14, 34). Consistent with these studies, the change from a low-salt (LS) diet (0.4%) to a high-salt (HS) diet (8%) for 21 days (21D) was coincident with a progressive elevation in MAP (113 ± 2 vs. 112 ± 2, 114 ± 4 vs. 122 ± 1, 116 ± 4 vs. 128 ± 1, 119 ± 4 vs.

146 ± 3, and 122 ± 4 vs. 172 ± 5 mmHg; LS vs. HS on *days 0, 3, 7, 14,* and *21* after a change of diet, $P <$ 0.05) (Fig. 1*A*) and albuminuria (1.31 ± 0.1 vs. 3.47 ± 0.33, 6.75 ± 1.27, 13.28 ± 2.14, and 17.04 ± 2.68 Alb/Cre ratio for LS vs. 3, 7, 14, and 21 days of HS, respectively, $P < 0.05$) (Fig. 1*B*). Interestingly, serum albumin levels were significantly reduced after 7 days HS and declined further thereafter (2.57 ± 0.07, 2.46 ± 0.08, and 2.44 ± 0.07 g/dl at 7D, 14D, and 21D of HS, respectively, vs. 2.98 ± 0.07 g/dl at LS, $P < 0.05$) (Fig. 1*C*). In contrast, serum concentration of globulins, blood proteins with significantly higher molecular weight and correspondingly lower permeability for glomeruli filtration barrier (3.16 ± 0.03 at LS vs. 2.76 ± 0.12, 3.07 ± 0.15, 3.3 ± 0.08, and 3.38 ± 0.12 g/dl at 7D, 14D, and 21D of HS) and creatinine (0.36 ± 0.03 at LS vs. 0.36 ± 0.04, 0.32 ± 0.03, 0.34 ± 0.03, and 0.38 ± 0.04 mg/dl at 7D, 14D, and 21D on HS correspondingly) was stable during the development of hypertension (Fig. 1, *D* and *E*). These data demonstrate the marked and progressive changes in albumin handling and serum albumin/globulin ratio, which might indicate pathological remodeling in kidney function during the development of hypertension.

High-salt diet increases glomerular permeability to albumin. To determine whether increased glomerular permeability to albumin causes albuminuria in SS rats fed a HS diet, we first evaluated the use of intravital two-photon microscopy (ITPM) as a means to investigate glomerular function in vivo. We found that the SS rats possess a superficial glomerular network, suggesting that our ITPM-based imaging approach would be a suitable means for examination. To monitor albumin handing in the kidney, superficial glomeruli were optically sectioned before and after intravenous infusion of Texas Red-labeled albumin (TR-albumin) following 2 wk of HS or LS diets (Supplemental Video S1; Supplemental Material for this article is available on the *AJP-Renal Physiology* web site). By measuring TR-albumin fluorescence in the glomerular capillaries and the Bowman's space, we derived a glomerular sieving coefficient for albumin (GSC_{alb}), as described previously (49). Previously reported values vary significantly, ranging from 0.08×10^{-3} to 0.07, depending on pathophysiological status and method used (37). Representative images reveal elevated albumin levels in the Bowman's capsule (Fig. 2*A*) as well as surrounding fibrosis and turbulent flow in the glomerular capillaries (Supplemental Video S2, *A* and *B*) after 14 days of HS diet. We found that the GSC_{alb} for LS-fed SS rats was 0.0146 ± 0.0015, which is consistent with measurements from Munich-Wistar rats (50). Using serum albumin and GFR values obtained for SS rats on the LS diet (14), GSC_{alb} corresponds to ~0.797 ± 0.084 g albumin/day filtered, as calculated similarly to previously described equations for mass balance of albumin filtration (65). Following consumption of a HS diet for 14 days, GSC_{alb} was increased 370%, correlating to ~3.689 ± 2.005 g albumin/day filtered (0.0146 ± 0.0015 vs. 0.0686 ± 0.0373, GSC_{alb} for LS vs. 14D on HS, respectively; $n \geq 5$ for each group, $P < 0.05$) (Fig. 2*B*).

To determine whether a HS diet affects glomerular permeability, we calculated albumin reflection coefficient (σ_{alb}), in ex vivo glomeruli using an assay based on changes in glomerular volume dynamics and fluorescent dilution (see Fig. 2*C* and Supplemental Video S3, *A* and *B*). Following ITPM, glomeruli were extracted and decapsulated, and permeability studies were performed by exposing isolated glomeruli to oncotic gradients. The oncotic pressure created by reducing bovine serum albumin (BSA) concentration in the recording chamber reestablished a transcapillary albumin gradient that was directly proportional to the relative permeability to albumin (P_{alb}) in the absence of hydraulic forces in isolated glomeruli. Consistent with results in vivo showing a significant elevation of GSC_{alb} in HS-fed rats, we found an impairment in the glomerular volume dynamics in HS-fed animals (120 ± 5 vs. 109 ± 4, 102 ± 2, and 106 ± 4% of maximum volume change; LS vs. 3, 7, and 14 days on HS, respectively; Fig. 2*D*). Additionally, the dilution of fluorescence in the glomerular capillaries due to water influx in response to the oncotic gradient was significantly reduced in the HS diet state (0.74 ± 0.02 vs. 0.79 ± 0.01, 0.86 ± 0.01, and 0.83 ± 0.01 FITC

AU; LS vs. 3, 7, and 14 days on HS, respectively; Fig. 2*E*). Corresponding changes in P_{alb} are shown in Fig. 2*F* (volume measurements on *days 3, 7,* and *14* of the HS diet are 0.07 ± 0.01, 0.15 ± 0.02, and 0.11 ± 0.02, $P < 0.05$ compared with LS; fluorescent measurements are 0.13 ± 0.03, 0.18 ± 0.02, and 0.16 ± 0.02, $P < 0.05$ compared with LS). Collectively, these data indicate that the integrity of the glomerular barrier in rats fed a HS diet is severely compromised by the changes in both glomerular hydrodynamics and permeability and may represent a causal mechanism for the ensuing rise in blood pressure.

Proximal tubular reabsorption is a contributing factor to albuminuria. It has been shown that both glomerular permeability and PT reabsorption of albumin play significant and likely interactive roles in determining albuminuria (17, 37). We next assessed by ITPM how PT responded to the increased filtered load of albumin following HS consumption (Fig. 3*A* and Supplementary Video S4). To determine the extent of albumin reabsorption in individual PTs, TR-albumin fluorescence was calculated at different time points for the 30-min period after TR-albumin was infused into blood stream. As shown in Fig. 3*B*, LS-fed SS rats reabsorbed a constant level of albumin (537 ± 32 vs. 532 ± 25 AU at 10- to 15- vs. 25- to 30-min intervals after TR-albumin infusion; $n \geq 27$ tubules for each group), suggesting a stable regulation of albumin uptake/transcytosis mechanisms for returning filtered albumin to the circulation, consistent with previous reports (65). In contrast, SS rats fed a HS diet began filtering more albumin (Fig. 2), which correlated with an increase in PT uptake of TR-albumin (532 ± 25 vs. 935 ± 77, $1,156 \pm 121$, and $1,088 \pm 62$ AU, LS vs. 3-, 7-, and 14-day HS, respectively, at 25- to 30-min intervals after TR-albumin infusion; $n \geq 10$ tubules for each group, $P < 0.05$ compared with LS) (Fig. 3, *B* and *C*).

In addition to increased PT reabsorption with the HS diet, we observed areas with high concentration of TR-albumin in PT (Figs. 4*A* and 5*B*). Most of the cells in PTs flooded with TR-albumin concentrate fluorescent dye on the apical side, which could indicate impaired transport mechanisms for albumin (Fig. 4*B*). The presence of granular casts in PT flooded with albumin was shown in vivo and during immunohystochemistry staining with Mason's trichrome for SS rat kidney cortex 14 days after a HS diet (Fig. 4, *A* and *C*). Overall, low magnification screening analysis of PT revealed damage of perivascular capillary bed (Fig. 5*A*), increased abundance of granular casts in the tubular lumen, apoptotic cell debris, dilation, and necrotic epithelial walls in HS-fed rats (Fig. 5, *B* and *C*). Immunohistochemistry staining of SS rats fed a HS diet further revealed the presence of PT casts in the kidney cortex (Fig. 5*D*). Cumulatively, these results indicate that PT albumin reuptake mechanisms and PT tubules conditions are significantly affected by prolonged HS consumption.

Microvascular changes associated with hypertension and renal damage. Hypertension increases the likelihood of heart failure and peripheral vascular disease, which is accompanied by a number of pathological changes in the vasculature, such as turbulent blood flow, microvascular occlusion, and disruption of the vascular wall. It was also demonstrated previously that the communication between PT and endothelial cells directly affects the function of adjacent peritubular blood vessels (31, 36). Because pathological damage to the PT and the surrounding capillaries (Fig. 5) can affect hemodynamic properties, blood flow through the capillaries as well as vascular diameter (VD) were measured by taking line scans in vivo during the development of salt-sensitive hypertension (Fig. 6, *A* and *B*). Following 7 days on a HS diet, the SS rats exhibited a significant increase in VD (13.3 ± 0.4 vs. 16 ± 0.4, 19.2 ± 0.4, and 17.6 ± 0.4 μm for LS, 3, 7, and 14 days on HS, respectively, $P < 0.05$, LS compared with 7- and 14-day HS) and an elevation in RBC velocity (771 ± 22.2 vs. 678.5 ± 22.2, 970.2 ± 125.5, and $1,039.9 \pm 71.8$ μm/s for LS and 3, 7, and 14 days on HS, respectively, $P < 0.05$, LS compared with HS), consistent with impaired autoregulatory mechanisms. In addition, we observed disruption of the vascular walls (vascular extravasation) in

hypertensive kidneys. The injection of the nonpermeable to the glomerular filtration barrier, 150-kDa, FITC-labeled dextran revealed a significant increase in the FITC in the interstitial space, which corresponded to the leakage of high-molecular weight dextran in SS rats fed a HS diet (0.61 ± 0.09 vs. 1.22 ± 0.14 for LS and 14-day HS, respectively, $P < 0.05$; [Fig. 6C](#)). Thus, it is likely that increased blood flow represents the consequence of PT and perivascular capillary bed damage and contributes to progression of the disease in the SS rat.

DISCUSSION

Salt-induced hypertension and the associated renal and cardiovascular complications affect a large population and are a major cause of CKD. The results presented here highlight the complex nature of the renal physiological changes that occur during hypertension and albuminuria. It is widely accepted that albuminuria is a strong predictor of renal damage and kidney disease. Albuminuria also plays a significant role in the pathogenesis of hypertension as well as other cardiovascular diseases, including congestive heart failure, metabolic syndrome, and CKD ([4](#), [13](#), [14](#), [38](#), [57](#)). According to the Framingham Heart Study, albuminuria was identified as an independent risk factor for cardiovascular disease even in the absence of other disease-specific markers ([25](#), [54](#), [57](#)). Clinically, albuminuria is considered a marker of widespread vascular damage in the hypertensive population and is among one of the clinical parameters associated with poor outcomes ([9](#)).

Despite the significance of albuminuria in hypertension, the events leading to albuminuria are not well understood. The goal of the current study was to determine the mechanisms contributing to albuminuria in the kidney of the Dahl SS rat, a rat model of salt-sensitive hypertension. Upon high salt consumption we observed significant changes in blood pressure and albumin handling in the kidney. Interestingly, the hypertensive rat's serum albumin levels were significantly lower than those of normotensive rats. These observations are consistent with recent clinical studies ([59](#)), indicating that serum albumin was significantly lower in patients with clinically overt cardiovascular disease. In vivo analysis during HS consumption revealed that in addition to increased glomerular permeability to albumin, PT reabsorption mechanisms were also augmented, which likely represent a compensatory mechanism due to increased filtration of albumin. These results suggest that both the glomeruli and PT epithelial cells play significant roles in regulating albuminuria and kidney function during hypertension.

Previous findings have attributed albuminuria to either glomerular or PT damage, but concurrent analysis of both factors has, to the best of our knowledge, not been carried out ([7](#), [65](#)). In this study, we used ITPM imaging of the kidney to quantitatively analyze the intrarenal mechanisms involved in the control of blood pressure and albumin handling in the context of salt-mediated hypertension. The same imaging technique was previously applied to studying different disease states in Munich-Wistar rats ([49](#), [60](#)), demonstrating its validity and applicability. By applying this methodology, we found that the HS diet caused a marked increase in albumin filtration in the SS rat [3.7 (HS) vs. 0.8 g albumin/day (LS), $P < 0.05$; [Fig. 2B](#)]. Complementary studies of glomerular hemodynamics in vitro showed that glomeruli isolated from rats fed a HS diet exhibited increased glomerular permeability to albumin and impaired the responsiveness to the oncotic gradient changes. Although we observed changes in glomerular function, we also observed a concomitant increase in PT reabsorption of albumin. These findings suggest that as albumin filtration increases in HS-fed rats, the PT attempts to compensate by actively reabsorbing albumin in all PT segments ([Figs. 3B](#) and [4A](#)). Although this protects acutely (3 days HS) against albuminuria development, our data show that the PT quickly becomes overwhelmed and albumin reuptake markedly declines. After 14 days of

the HS diet, we also observed severe pathological changes, including the presence of cast material and necrotic lesions (Fig. 5). Collectively, these results suggest that both the glomerulus and the PT are contributing to albuminuria and renal damage.

Numerous clinical reports indicate that the main contributor to the progression of CKD is the PT (10, 28, 42). To maintain glomerulotubular balance during CKD, tubular reabsorption mechanisms must compensate for changes in filtration (55). This increase in PT metabolic load can have detrimental effects, including a rapid increase in reactive oxygen species production (56), tubular cell apoptosis, fibrosis, and nephron loss (55, 62). Our data are consistent with these findings and suggest that the PT are likely being directly affected by the changes in glomerular filtration. Although there is a direct implication of the PT in Fanconi Syndrome (40), the data presented here and by others previously support the conclusion that the PT plays a significant role in the pathogenesis of CKD.

Despite previous findings (50), the renal albumin handling and transcytosis in PT cells is still debatable. Multiple studies, including experiments with knockout animals, showed the importance of proteins regulating PT albumin reuptake, such as megalin and cubilin (2, 12, 29, 43). However, there is no evidence of changes in the abundance of these reuptake proteins or the distribution in PT cells during albuminuria or proteinuria (65). Recent findings suggest a possible molecular mechanism of albumin transport through the neonatal Fc receptor (FcRn) which is expressed in the apical region of PT cells (66). Additional studies investigating the abundance and function of FcRn and other proteins during CKD and albuminuria will be needed to uncover the mechanisms by which albumin is handled in the PT.

Microalbuminuria has been associated with endothelial damage and is an independent risk factor associated with diabetes, CKD, hypertension, venous thromboembolism, and all-cause mortality (30). Fundamental studies by Brenner (8) have suggested that glomerulotubular balance is maintained by intrinsic tubular and peritubular capillary adaptations that parallel the filtration rate of nephron. Thus, in addition to changes in glomerular permeability and PT reabsorption, we attempted to determine the contribution of vascular hemodynamic properties to albuminuria. Sampling of renal vessels throughout the cortex revealed that vascular flow rate and diameter increase upon HS consumption (Fig. 6A). These changes are contradictory to the normal physiological response of the blood vessels and support the previous observations indicating that autoregulatory mechanisms are impaired in the SS rat (21, 27). Because blood flow to the glomerulus is not maintained at a constant rate, this may partially explain the changes in glomerular permeability to albumin and GFR that occur following HS consumption. Furthermore, in vivo studies (31, 32) utilizing target bacterial infections of PT cells indicate that disruption in tubulovascular cross-talk within hours results in ischemia of surrounding capillaries and further triggers endothelial cell damage and loss of renal microvascular integrity. In addition, genetic ablation of tubular vascular endothelial growth factor A results in selective dropout of peritubular microvessels, which indicates tide relation between tubular and perivascular regions of the kidneys (18). Similarly, our data indicate significant changes in perivascular beds during PT damage (Figs. 5A and 6C). Impaired microvascular blood flow can lead to substantial differences in oxygen tension and contribute to the development of vascular damage, which is highly important from the clinical point since, in comparison with tubular epithelial cells, the regenerative capacity of endothelial cells is limited (5, 19).

There is a clear association between the infiltration of immune cells in the kidney and hypertension and renal damage in patients, but the mechanistic relationship is not well defined (64). It has been suggested that immune cell infiltrates may invoke a change in blood pressure and renal function as early as 4–8 days post-initiation of a HS diet (16, 35). It is possible to track immune cells in vivo by filtering scans for nuclear

Hoechst staining (Fig. 6B). Future studies utilizing genetic approaches to selectively label leukocyte subpopulations via genetic reporters will be needed to elucidate the specific immune mechanisms contributing to salt-sensitive hypertension.

Although ITPM allows for in vivo imaging of the cortex renal function, it relies on the premise and potential limitation that the animal model's kidney contains superficial glomeruli for measuring glomerular sieving coefficients. Many of the previous studies of renal function, especially those utilizing the micropuncture approach (58), were performed in Munich-Wistar Rats, which contain large numbers of superficial glomeruli. As indicated here, the SS rat kidneys contain some but not many superficial glomeruli, which allowed us to explore mechanisms regulating albumin handling and associated pathological changes during the development of salt-sensitive hypertension. It is likely that both the cortex and medulla are contributing to the pathogenesis of hypertension in the Dahl SS rats, since it was shown previously that the percentages of injured cortical and juxtamedullary glomeruli are equal during the development of salt-induced hypertension in SS rats (39). Moreover, a mixture of superficial, cortical, and juxtamedullary glomeruli was used in this study for ex vivo permeability assay.

Antihypertensive therapy typically involves inhibition of the angiotensin system and is effective as a first-pass treatment option. However, mild renal insufficiency remains present in a significant proportion of hypertensive patients undergoing treatment (46). This is coincident with a marked increase in cardiovascular disease risk, including stroke, coronary artery disease, heart failure, atrial fibrillation, and peripheral vascular disease (3, 45). Clinical treatment of albuminuria includes the use of ACE inhibitors and ARBs, which mostly exert their effects on the glomeruli and the vasculature within the kidney. Interestingly, our data show that, even during the early stages of salt-sensitive hypertension, severe damage occurs in the PT, resulting in pathological changes and attenuated albumin transport. Thus, therapies designed to mitigate PT pathology and promote its repair and regeneration may be a complementary treatment option (10). Further understanding of the pharmacological prevention of PT damage during the development of hypertension is essential for treating albuminuria and maintaining renal function.

GRANTS

DISCLOSURES

No conflicts of interest, financial or otherwise, are declared by the authors.

AUTHOR CONTRIBUTIONS

B.T.E., A.S., B.A.M., A.M.G., and O.P. conceived and designed research; B.T.E., R.M.S., G.J.R., S.B.C.-B., and O.P. performed experiments; B.T.E., R.M.S., M.M.K., and O.P. analyzed data; B.T.E., R.M.S., G.J.R., S.B.C.-B., M.M.K., A.S., B.A.M., and O.P. interpreted results of experiments; B.T.E., C.M.-R., A.S., A.M.G., and O.P. drafted manuscript; B.T.E., C.M.-R., A.S., B.A.M., A.M.G., and O.P. edited and revised manuscript; B.T.E., R.M.S., G.J.R., S.B.C.-B., M.M.K., C.M.-R., A.S., B.A.M., A.M.G., and O.P.

approved final version of manuscript; O.P. prepared figures.

Supplementary Material

Supplemental_Video_1.avi:

Supplemental_Video_2A.avi:

Supplemental_Video_2B.avi:

Supplemental_Video_3A.avi:

Supplemental_Video_3B.avi:

Supplemental_Video_4.avi:

ACKNOWLEDGMENTS

REFERENCES

1. Alani H, Tamimi A, Tamimi N. Cardiovascular co-morbidity in chronic kidney disease: Current knowledge and future research needs. World J Nephrol 3: 156–168, 2014. doi:10.5527/wjn.v3.i4.156. [PMCID: PMC4220348] [PubMed: 25374809] [CrossRef: 10.5527/wjn.v3.i4.156]

2. Amsellem S, Gburek J, Hamard G, Nielsen R, Willnow TE, Devuyst O, Nexo E, Verroust PJ, Christensen EI, Kozyraki R. Cubilin is essential for albumin reabsorption in the renal proximal tubule. J Am Soc Nephrol 21: 1859–1867, 2010. doi:10.1681/ASN.2010050492. [PMCID: PMC3014001] [PubMed: 20798259] [CrossRef: 10.1681/ASN.2010050492]

3. Angeli F, Reboldi G, Verdecchia P. Hypertension, inflammation and atrial fibrillation. J Hypertens 32: 480–483, 2014. doi:10.1097/HJH.0000000000000112. [PubMed: 24477094] [CrossRef: 10.1097/HJH.0000000000000112]

4. Bakris GL, Kuritzky L. Monitoring and managing urinary albumin excretion: practical advice for primary care clinicians. Postgrad Med 121: 51–60, 2009. doi:10.3810/pgm.2009.07.2031. [PubMed: 19641270] [CrossRef: 10.3810/pgm.2009.07.2031]

5. Basile DP, Friedrich JL, Spahic J, Knipe N, Mang H, Leonard EC, Changizi-Ashtiyani S, Bacallao RL, Molitoris BA, Sutton TA. Impaired endothelial proliferation and mesenchymal transition contribute to vascular rarefaction following acute kidney injury. Am J Physiol Renal Physiol 300: F721–F733, 2011. doi:10.1152/ajprenal.00546.2010. [PMCID: PMC3064142] [PubMed: 21123492] [CrossRef: 10.1152/ajprenal.00546.2010]

6. Bolisetty S, Agarwal A. Urine albumin as a biomarker in acute kidney injury. Am J Physiol Renal Physiol 300: F626–F627, 2011. doi:10.1152/ajprenal.00004.2011. [PMCID: PMC3064133] [PubMed: 21228105] [CrossRef: 10.1152/ajprenal.00004.2011]

7. Brasen JC, Burford JL, McDonough AA, Holstein-Rathlou NH, Peti-Peterdi J. Local pH domains regulate NHE3-mediated Na$^+$ reabsorption in the renal proximal tubule. Am J Physiol Renal Physiol 307: F1249–F1262, 2014. doi:10.1152/ajprenal.00174.2014. [PMCID: PMC4254968] [PubMed: 25298526] [CrossRef: 10.1152/ajprenal.00174.2014]

8. Brenner BM. Nephron adaptation to renal injury or ablation. Am J Physiol 249: F324–F337, 1985. [PubMed: 3898871]

9. Bruno RM, Daghini E, Versari D, Sgrò M, Sanna M, Venturini L, Romanini C, Di Paco I, Sudano I, Cioni R, Lerman LO, Ghiadoni L, Taddei S, Pinto S. Predictive role of renal resistive index for clinical outcome after revascularization in hypertensive patients with atherosclerotic renal artery stenosis: a monocentric observational study. Cardiovasc Ultrasound 12: 9, 2014. doi:10.1186/1476-7120-12-9. [PMCID: PMC3937242] [PubMed: 24555729] [CrossRef: 10.1186/1476-7120-12-9]

10. Chevalier RL. The proximal tubule is the primary target of injury and progression of kidney disease: role of the glomerulotubular junction. Am J Physiol Renal Physiol 311: F145–F161, 2016. doi:10.1152/ajprenal.00164.2016. [PMCID: PMC4967168] [PubMed: 27194714] [CrossRef: 10.1152/ajprenal.00164.2016]

11. Choong FX, Sandoval RM, Molitoris BA, Richter-Dahlfors A. Multiphoton microscopy applied for real-time intravital imaging of bacterial infections in vivo. Methods Enzymol 506: 35–61, 2012. doi:10.1016/B978-0-12-391856-7.00027-5. [PMCID: PMC4136485] [PubMed: 22341218] [CrossRef: 10.1016/B978-0-12-391856-7.00027-5]

12. Christensen EI, Birn H. Megalin and cubilin: synergistic endocytic receptors in renal proximal tubule. Am J Physiol Renal Physiol 280: F562–F573, 2001. [PubMed: 11249847]

13. Comper WD, Hilliard LM, Nikolic-Paterson DJ, Russo LM. Disease-dependent mechanisms of albuminuria. Am J Physiol Renal Physiol 295: F1589–F1600, 2008. doi:10.1152/ajprenal.00142.2008. [PubMed: 18579704] [CrossRef: 10.1152/ajprenal.00142.2008]

14. Cowley AW Jr, Ryan RP, Kurth T, Skelton MM, Schock-Kusch D, Gretz N. Progression of glomerular filtration rate reduction determined in conscious Dahl salt-sensitive hypertensive rats. Hypertension 62: 85–90, 2013. doi:10.1161/HYPERTENSIONAHA.113.01194. [PMCID: PMC3806646] [PubMed: 23630946] [CrossRef: 10.1161/HYPERTENSIONAHA.113.01194]

15. de Jong PE, Curhan GC. Screening, monitoring, and treatment of albuminuria: Public health perspectives. J Am Soc Nephrol 17: 2120–2126, 2006. doi:10.1681/ASN.2006010097. [PubMed: 16825331] [CrossRef: 10.1681/ASN.2006010097]

16. De Miguel C, Das S, Lund H, Mattson DL. T lymphocytes mediate hypertension and kidney damage in Dahl salt-sensitive rats. Am J Physiol Regul Integr Comp Physiol 298: R1136–R1142, 2010. doi:10.1152/ajpregu.00298.2009. [PMCID: PMC2853394] [PubMed: 20147611] [CrossRef: 10.1152/ajpregu.00298.2009]

17. Dickson LE, Wagner MC, Sandoval RM, Molitoris BA. The proximal tubule and albuminuria: really! J

Am Soc Nephrol 25: 443–453, 2014. doi:10.1681/ASN.2013090950. [PMCID: PMC3935594] [PubMed: 24408874] [CrossRef: 10.1681/ASN.2013090950]

18. Dimke H, Sparks MA, Thomson BR, Frische S, Coffman TM, Quaggin SE. Tubulovascular cross-talk by vascular endothelial growth factor a maintains peritubular microvasculature in kidney. J Am Soc Nephrol 26: 1027–1038, 2015. doi:10.1681/ASN.2014010060. [PMCID: PMC4413754] [PubMed: 25385849] [CrossRef: 10.1681/ASN.2014010060]

19. Dimmeler S, Assmus B, Hermann C, Haendeler J, Zeiher AM. Fluid shear stress stimulates phosphorylation of Akt in human endothelial cells: involvement in suppression of apoptosis. Circ Res 83: 334–341, 1998. doi:10.1161/01.RES.83.3.334. [PubMed: 9710127] [CrossRef: 10.1161/01.RES.83.3.334]

20. Fan F, Chen CC, Zhang J, Schreck CM, Roman EA, Williams JM, Hirata T, Sharma M, Beard DA, Savin VJ, Roman RJ. Fluorescence dilution technique for measurement of albumin reflection coefficient in isolated glomeruli. Am J Physiol Renal Physiol 309: F1049–F1059, 2015. doi:10.1152/ajprenal.00311.2015. [PMCID: PMC4683305] [PubMed: 26447220] [CrossRef: 10.1152/ajprenal.00311.2015]

21. Fan F, Geurts AM, Murphy SR, Pabbidi MR, Jacob HJ, Roman RJ. Impaired myogenic response and autoregulation of cerebral blood flow is rescued in CYP4A1 transgenic Dahl salt-sensitive rat. Am J Physiol Regul Integr Comp Physiol 308: R379–R390, 2015. doi:10.1152/ajpregu.00256.2014. [PMCID: PMC4346760] [PubMed: 25540098] [CrossRef: 10.1152/ajpregu.00256.2014]

22. Ilatovskaya DV, Palygin O, Levchenko V, Endres BT, Staruschenko A. The Role of Angiotensin II in Glomerular Volume Dynamics and Podocyte Calcium Handling. Sci Rep 7: 299, 2017. doi:10.1038/s41598-017-00406-2. [PMCID: PMC5428415] [PubMed: 28331185] [CrossRef: 10.1038/s41598-017-00406-2]

23. Ilatovskaya DV, Palygin O, Levchenko V, Staruschenko A. Single-channel analysis and calcium imaging in the podocytes of the freshly isolated glomeruli. J Vis Exp 100: e52850, 2015. doi:10.3791/52850. [PMCID: PMC4544950] [PubMed: 26167808] [CrossRef: 10.3791/52850]

24. Jaradat MI, Molitoris BA. Cardiovascular disease in patients with chronic kidney disease. Semin Nephrol 22: 459–473, 2002. doi:10.1053/snep.2002.35964. [PubMed: 12430090] [CrossRef: 10.1053/snep.2002.35964]

25. Jarraya F, Lakhdar R, Kammoun K, Mahfoudh H, Drissa H, Kammoun S, Abid M, Hachicha J. Microalbuminuria: a useful marker of cardiovascular disease. Iran J Kidney Dis 7: 178–186, 2013. [PubMed: 23689147]

26. Johnson DW, Jones GR, Mathew TH, Ludlow MJ, Chadban SJ, Usherwood T, Polkinghorne K, Colagiuri S, Jerums G, Macisaac R, Martin H; Australasian Proteinuria Consensus Working Group . Chronic kidney disease and measurement of albuminuria or proteinuria: a position statement. Med J Aust 197: 224–225, 2012. doi:10.5694/mja11.11468. [PubMed: 22900872] [CrossRef: 10.5694/mja11.11468]

27. Karlsen FM, Andersen CB, Leyssac PP, Holstein-Rathlou NH. Dynamic autoregulation and renal injury in Dahl rats. Hypertension 30: 975–983, 1997. doi:10.1161/01.HYP.30.4.975. [PubMed: 9336403] [CrossRef: 10.1161/01.HYP.30.4.975]

28. Klinkhammer BM, Goldschmeding R, Floege J, Boor P. Treatment of Renal Fibrosis-Turning Challenges into Opportunities. Adv Chronic Kidney Dis 24: 117–129, 2017. doi:10.1053/j.ackd.2016.11.002. [PubMed: 28284377] [CrossRef: 10.1053/j.ackd.2016.11.002]

29. Leheste JR, Rolinski B, Vorum H, Hilpert J, Nykjaer A, Jacobsen C, Aucouturier P, Moskaug JO, Otto A, Christensen EI, Willnow TE. Megalin knockout mice as an animal model of low molecular weight proteinuria. Am J Pathol 155: 1361–1370, 1999. doi:10.1016/S0002-9440(10)65238-8. [PMCID: PMC1867027] [PubMed: 10514418] [CrossRef: 10.1016/S0002-9440(10)65238-8]

30. Mahmoodi BK, Gansevoort RT, Veeger NJ, Matthews AG, Navis G, Hillege HL, van der Meer J; Prevention of Renal and Vascular End-stage Disease (PREVEND) Study Group . Microalbuminuria and risk of venous thromboembolism. JAMA 301: 1790–1797, 2009. doi:10.1001/jama.2009.565. [PubMed: 19417196] [CrossRef: 10.1001/jama.2009.565]

31. Månsson LE, Melican K, Boekel J, Sandoval RM, Hautefort I, Tanner GA, Molitoris BA, Richter-Dahlfors A. Real-time studies of the progression of bacterial infections and immediate tissue responses in live animals. Cell Microbiol 9: 413–424, 2007. doi:10.1111/j.1462-5822.2006.00799.x. [PubMed: 16953802] [CrossRef: 10.1111/j.1462-5822.2006.00799.x]

32. Månsson LE, Melican K, Molitoris BA, Richter-Dahlfors A. Progression of bacterial infections studied in real time—novel perspectives provided by multiphoton microscopy. Cell Microbiol 9: 2334–2343, 2007. doi:10.1111/j.1462-5822.2007.01019.x. [PubMed: 17662072] [CrossRef: 10.1111/j.1462-5822.2007.01019.x]

33. Mattson DL, Dwinell MR, Greene AS, Kwitek AE, Roman RJ, Jacob HJ, Cowley AW Jr. Chromosome substitution reveals the genetic basis of Dahl salt-sensitive hypertension and renal disease. Am J Physiol Renal Physiol 295: F837–F842, 2008. doi:10.1152/ajprenal.90341.2008. [PMCID: PMC2536867] [PubMed: 18653478] [CrossRef: 10.1152/ajprenal.90341.2008]

34. Mattson DL, Kunert MP, Kaldunski ML, Greene AS, Roman RJ, Jacob HJ, Cowley AW Jr. Influence of diet and genetics on hypertension and renal disease in Dahl salt-sensitive rats. Physiol Genomics 16: 194–203, 2004. doi:10.1152/physiolgenomics.00151.2003. [PubMed: 14600213] [CrossRef: 10.1152/physiolgenomics.00151.2003]

35. Mattson DL, Lund H, Guo C, Rudemiller N, Geurts AM, Jacob H. Genetic mutation of recombination activating gene 1 in Dahl salt-sensitive rats attenuates hypertension and renal damage. Am J Physiol Regul Integr Comp Physiol 304: R407–R414, 2013. doi:10.1152/ajpregu.00304.2012. [PMCID: PMC3602820] [PubMed: 23364523] [CrossRef: 10.1152/ajpregu.00304.2012]

36. Melican K, Sandoval RM, Kader A, Josefsson L, Tanner GA, Molitoris BA, Richter-Dahlfors A. Uropathogenic Escherichia coli P and Type 1 fimbriae act in synergy in a living host to facilitate renal colonization leading to nephron obstruction. PLoS Pathog 7: e1001298, 2011. doi:10.1371/journal.ppat.1001298. [PMCID: PMC3044688] [PubMed: 21383970] [CrossRef: 10.1371/journal.ppat.1001298]

37. Molitoris BA. Using 2-photon microscopy to understand albuminuria. Trans Am Clin Climatol Assoc 125: 343–356, 2014. [PMCID: PMC4112674] [PubMed: 25125750]

38. Molitoris BA. Yet another advance in understanding albuminuria? J Am Soc Nephrol 21: 2013–2015, 2010. doi:10.1681/ASN.2010101075. [PubMed: 21051742] [CrossRef: 10.1681/ASN.2010101075]

39. Mori T, Polichnowski A, Glocka P, Kaldunski M, Ohsaki Y, Liang M, Cowley AW Jr. High perfusion pressure accelerates renal injury in salt-sensitive hypertension. J Am Soc Nephrol 19: 1472–1482, 2008.

doi:10.1681/ASN.2007121271. [PMCID: PMC2488259] [PubMed: 18417720] [CrossRef: 10.1681/ASN.2007121271]

40. Norden AG, Lapsley M, Igarashi T, Kelleher CL, Lee PJ, Matsuyama T, Scheinman SJ, Shiraga H, Sundin DP, Thakker RV, Unwin RJ, Verroust P, Moestrup SK. Urinary megalin deficiency implicates abnormal tubular endocytic function in Fanconi syndrome. J Am Soc Nephrol 13: 125–133, 2002. [PubMed: 11752029]

41. O'Toole JF, Sedor JR. Kidney disease: new technologies translate mechanisms to cure. J Clin Invest 124: 2294–2298, 2014. doi:10.1172/JCI76825. [PMCID: PMC4089455] [PubMed: 24892702] [CrossRef: 10.1172/JCI76825]

42. Perazella MA. Clinical Approach to Diagnosing Acute and Chronic Tubulointerstitial Disease. Adv Chronic Kidney Dis 24: 57–63, 2017. doi:10.1053/j.ackd.2016.08.003. [PubMed: 28284380] [CrossRef: 10.1053/j.ackd.2016.08.003]

43. Pohl M, Kaminski H, Castrop H, Bader M, Himmerkus N, Bleich M, Bachmann S, Theilig F. Intrarenal renin angiotensin system revisited: role of megalin-dependent endocytosis along the proximal nephron. J Biol Chem 285: 41935–41946, 2010. doi:10.1074/jbc.M110.150284. [PMCID: PMC3009920] [PubMed: 20966072] [CrossRef: 10.1074/jbc.M110.150284]

44. Presson RG Jr, Brown MB, Fisher AJ, Sandoval RM, Dunn KW, Lorenz KS, Delp EJ, Salama P, Molitoris BA, Petrache I. Two-photon imaging within the murine thorax without respiratory and cardiac motion artifact. Am J Pathol 179: 75–82, 2011. doi:10.1016/j.ajpath.2011.03.048. [PMCID: PMC3123791] [PubMed: 21703395] [CrossRef: 10.1016/j.ajpath.2011.03.048]

45. Rapsomaniki E, Timmis A, George J, Pujades-Rodriguez M, Shah AD, Denaxas S, White IR, Caulfield MJ, Deanfield JE, Smeeth L, Williams B, Hingorani A, Hemingway H. Blood pressure and incidence of twelve cardiovascular diseases: lifetime risks, healthy life-years lost, and age-specific associations in 1·25 million people. Lancet 383: 1899–1911, 2014. doi:10.1016/S0140-6736(14)60685-1. [PMCID: PMC4042017] [PubMed: 24881994] [CrossRef: 10.1016/S0140-6736(14)60685-1]

46. Ruilope LM. The kidney as a sensor of cardiovascular risk in essential hypertension. J Am Soc Nephrol 13, Suppl 3: S165–S168, 2002. doi:10.1097/01.ASN.0000034496.63958.F8. [PubMed: 12466307] [CrossRef: 10.1097/01.ASN.0000034496.63958.F8]

47. Saleh MA, Boesen EI, Pollock JS, Savin VJ, Pollock DM. Endothelin-1 increases glomerular permeability and inflammation independent of blood pressure in the rat. Hypertension 56: 942–949, 2010. doi:10.1161/HYPERTENSIONAHA.110.156570. [PMCID: PMC2959121] [PubMed: 20823379] [CrossRef: 10.1161/HYPERTENSIONAHA.110.156570]

48. Sandoval RM, Molitoris BA. Quantifying endocytosis in vivo using intravital two-photon microscopy. Methods Mol Biol 440: 389–402, 2008. doi:10.1007/978-1-59745-178-9_28. [PubMed: 18369960] [CrossRef: 10.1007/978-1-59745-178-9_28]

49. Sandoval RM, Molitoris BA. Quantifying glomerular permeability of fluorescent macromolecules using 2-photon microscopy in Munich Wistar rats. J Vis Exp 74: e50052, 2013. doi:10.3791/50052. [PMCID: PMC3664960] [PubMed: 23628966] [CrossRef: 10.3791/50052]

50. Sandoval RM, Wagner MC, Patel M, Campos-Bilderback SB, Rhodes GJ, Wang E, Wean SE,

Clendenon SS, Molitoris BA. Multiple factors influence glomerular albumin permeability in rats. J Am Soc Nephrol 23: 447–457, 2012. doi:10.1681/ASN.2011070666. [PMCID: PMC3294301] [PubMed: 22223875] [CrossRef: 10.1681/ASN.2011070666]

51. Sarnak MJ, Levey AS, Schoolwerth AC, Coresh J, Culleton B, Hamm LL, McCullough PA, Kasiske BL, Kelepouris E, Klag MJ, Parfrey P, Pfeffer M, Raij L, Spinosa DJ, Wilson PW; American Heart Association Councils on Kidney in Cardiovascular Disease, High Blood Pressure Research, Clinical Cardiology, and Epidemiology and Prevention . Kidney disease as a risk factor for development of cardiovascular disease: a statement from the American Heart Association Councils on Kidney in Cardiovascular Disease, High Blood Pressure Research, Clinical Cardiology, and Epidemiology and Prevention. Circulation 108: 2154–2169, 2003. doi:10.1161/01.CIR.0000095676.90936.80. [PubMed: 14581387] [CrossRef: 10.1161/01.CIR.0000095676.90936.80]

52. Savin VJ, Sharma R, Lovell HB, Welling DJ. Measurement of albumin reflection coefficient with isolated rat glomeruli. J Am Soc Nephrol 3: 1260–1269, 1992. [PubMed: 1477322]

53. Schießl IM, Hammer A, Riquier-Brison A, Peti-Peterdi J. Just look! Intravital microscopy as the best means to study kidney cell death dynamics. Semin Nephrol 36: 220–236, 2016. doi:10.1016/j.semnephrol.2016.03.009. [PMCID: PMC5425152] [PubMed: 27339387] [CrossRef: 10.1016/j.semnephrol.2016.03.009]

54. Schmieder RE, Schutte R, Schumacher H, Böhm M, Mancia G, Weber MA, McQueen M, Teo K, Yusuf S; ONTARGET/TRANSCEND investigators . Mortality and morbidity in relation to changes in albuminuria, glucose status and systolic blood pressure: an analysis of the ONTARGET and TRANSCEND studies. Diabetologia 57: 2019–2029, 2014. doi:10.1007/s00125-014-3330-9. ONTARGET/TRANSCEND investigators. [PubMed: 25037746] [CrossRef: 10.1007/s00125-014-3330-9]

55. Schnaper HW. The Tubulointerstitial Pathophysiology of Progressive Kidney Disease. Adv Chronic Kidney Dis 24: 107–116, 2017. doi:10.1053/j.ackd.2016.11.011. [PMCID: PMC5351778] [PubMed: 28284376] [CrossRef: 10.1053/j.ackd.2016.11.011]

56. Shalamanova L, McArdle F, Amara AB, Jackson MJ, Rustom R. Albumin overload induces adaptive responses in human proximal tubular cells through oxidative stress but not via angiotensin II type 1 receptor. Am J Physiol Renal Physiol 292: F1846–F1857, 2007. doi:10.1152/ajprenal.00265.2006. [PubMed: 17327499] [CrossRef: 10.1152/ajprenal.00265.2006]

57. Stephen R, Jolly SE, Nally JV Jr, Navaneethan SD. Albuminuria: when urine predicts kidney and cardiovascular disease. Cleve Clin J Med 81: 41–50, 2014. doi:10.3949/ccjm.81a.13040. [PubMed: 24391106] [CrossRef: 10.3949/ccjm.81a.13040]

58. Stockand JD, Vallon V, Ortiz P. In vivo and ex vivo analysis of tubule function. Compr Physiol 2: 2495–2525, 2012. doi:10.1002/cphy.c100051. [PubMed: 23720256] [CrossRef: 10.1002/cphy.c100051]

59. Sun J, Axelsson J, Machowska A, Heimbürger O, Bárány P, Lindholm B, Lindström K, Stenvinkel P, Qureshi AR. Biomarkers of cardiovascular disease and mortality risk in patients with advanced CKD. Clin J Am Soc Nephrol 11: 1163–1172, 2016. doi:10.2215/CJN.10441015. [PMCID: PMC4934843] [PubMed: 27281698] [CrossRef: 10.2215/CJN.10441015]

60. Tanner GA, Sandoval RM, Dunn KW. Two-photon in vivo microscopy of sulfonefluorescein secretion in normal and cystic rat kidneys. Am J Physiol Renal Physiol 286: F152–F160, 2004.

doi:10.1152/ajprenal.00264.2003. [PubMed: 12965895] [CrossRef: 10.1152/ajprenal.00264.2003]

61. Tziakas D, Chalikias G, Kareli D, Tsigalou C, Risgits A, Kikas P, Makrygiannis D, Chatzikyriakou S, Kampouromiti G, Symeonidis D, Voudris V, Konstantinides S. Spot urine albumin to creatinine ratio outperforms novel acute kidney injury biomarkers in patients with acute myocardial infarction. Int J Cardiol 197: 48–55, 2015. doi:10.1016/j.ijcard.2015.06.019. [PubMed: 26113474] [CrossRef: 10.1016/j.ijcard.2015.06.019]

62. Vallon V. The proximal tubule in the pathophysiology of the diabetic kidney. Am J Physiol Regul Integr Comp Physiol 300: R1009–R1022, 2011. doi:10.1152/ajpregu.00809.2010. [PMCID: PMC3094037] [PubMed: 21228342] [CrossRef: 10.1152/ajpregu.00809.2010]

63. Viazzi F, Pontremoli R. Blood pressure, albuminuria and renal dysfunction: the 'chicken or egg' dilemma. Nephrol Dial Transplant 29: 1453–1455, 2014. doi:10.1093/ndt/gfu183. [PubMed: 24811230] [CrossRef: 10.1093/ndt/gfu183]

64. Wade B, Abais-Battad JM, Mattson DL. Role of immune cells in salt-sensitive hypertension and renal injury. Curr Opin Nephrol Hypertens 25: 22–27, 2016. doi:10.1097/MNH.0000000000000183. [PMCID: PMC4724875] [PubMed: 26575395] [CrossRef: 10.1097/MNH.0000000000000183]

65. Wagner MC, Campos-Bilderback SB, Chowdhury M, Flores B, Lai X, Myslinski J, Pandit S, Sandoval RM, Wean SE, Wei Y, Satlin LM, Wiggins RC, Witzmann FA, Molitoris BA. Proximal tubules have the capacity to regulate uptake of albumin. J Am Soc Nephrol 27: 482–494, 2016. doi:10.1681/ASN.2014111107. [PMCID: PMC4731114] [PubMed: 26054544] [CrossRef: 10.1681/ASN.2014111107]

66. Wagner MC, Myslinski J, Pratap S, Flores B, Rhodes G, Campos-Bilderback SB, Sandoval RM, Kumar S, Patel M, Ashish, Molitoris BA. Mechanism of increased clearance of glycated albumin by proximal tubule cells. Am J Physiol Renal Physiol 310: F1089–F1102, 2016. doi:10.1152/ajprenal.00605.2015. [PMCID: PMC4889321] [PubMed: 26887834] [CrossRef: 10.1152/ajprenal.00605.2015]

67. Yan P, Zhu X, Li H, Shrubsole MJ, Shi H, Zhang MZ, Harris RC Jr, Hao CM, Dai Q. Association of high blood pressure with renal insufficiency: role of albuminuria, from NHANES, 1999-2006. PLoS One 7: e37837, 2012. doi:10.1371/journal.pone.0037837. [PMCID: PMC3388992] [PubMed: 22802927] [CrossRef: 10.1371/journal.pone.0037837]

Figures and Tables

Fig. 1.
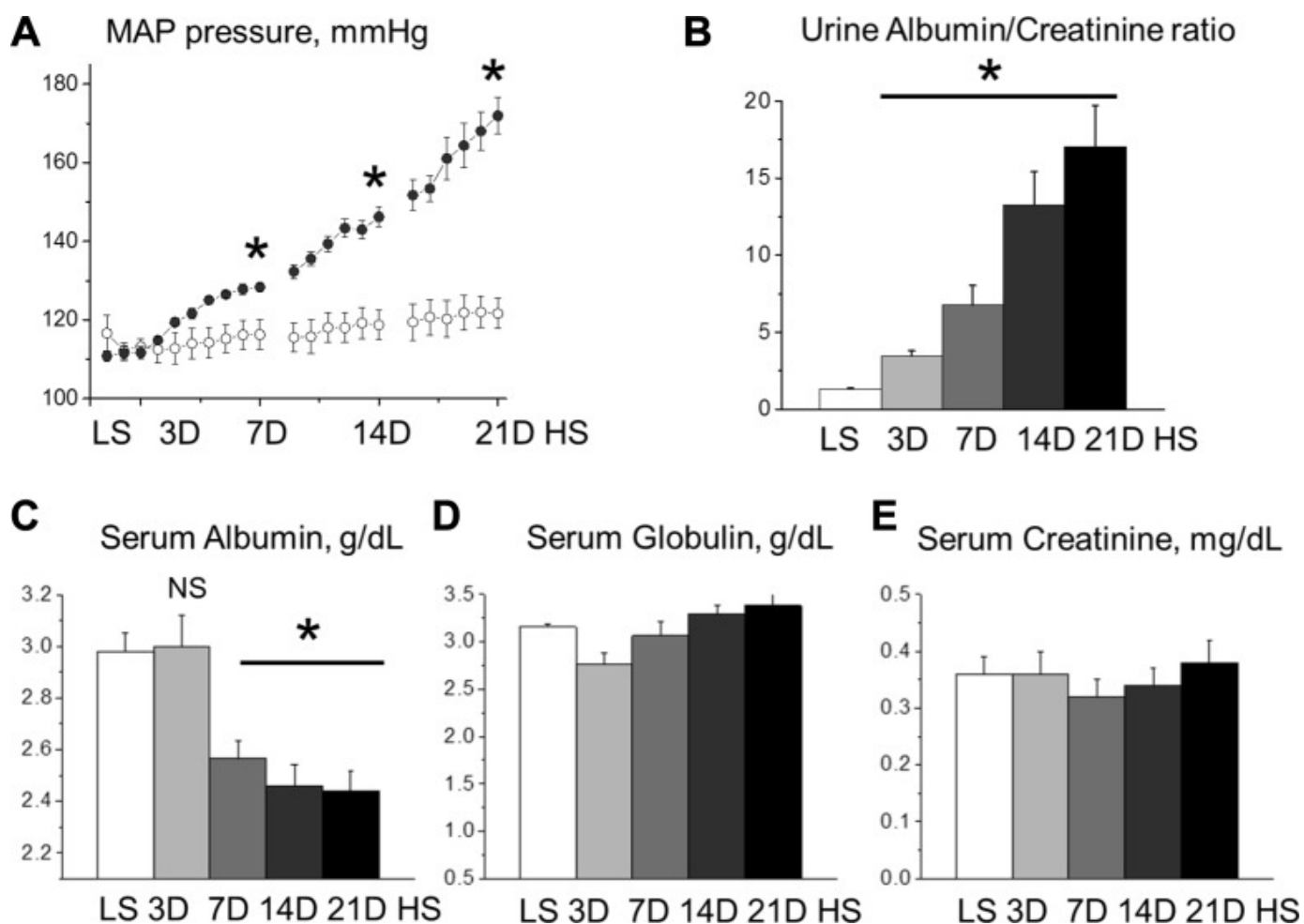
Development of salt-sensitive hypertension in Dahl salt-sensitive (SS) rats. *A*: mean arterial pressure (MAP) was measured by telemetry in SS rats fed low-salt (LS) followed by high-salt (HS) chow (0.4 vs. 8% NaCl, respectively). *B*: urine albumin/creatinine ratios demonstrate a rapid development of albuminuria in SS rats fed a HS diet. *C*: plasma albumin (68 kDa) level in SS rats fed a LS and HS diets, as shown in *A*. *D*: concentration of plasma globulins (92–120 kDa) during the development of salt-sensitive hypertension. *E*: serum creatinine level in SS rats fed LS and HS diet [3 (3D), 7 (7D), 14 (14D), and 21 days (21D)]; $n \geq 7$ rats/group for all graphs. *$P < 0.05$ compared with LS. NS, nonignificant. ○, MAP on the LS diet (NaCl 0.4%); ●, MAPS on HS (NaCl 8%) diets.

Fig. 2.
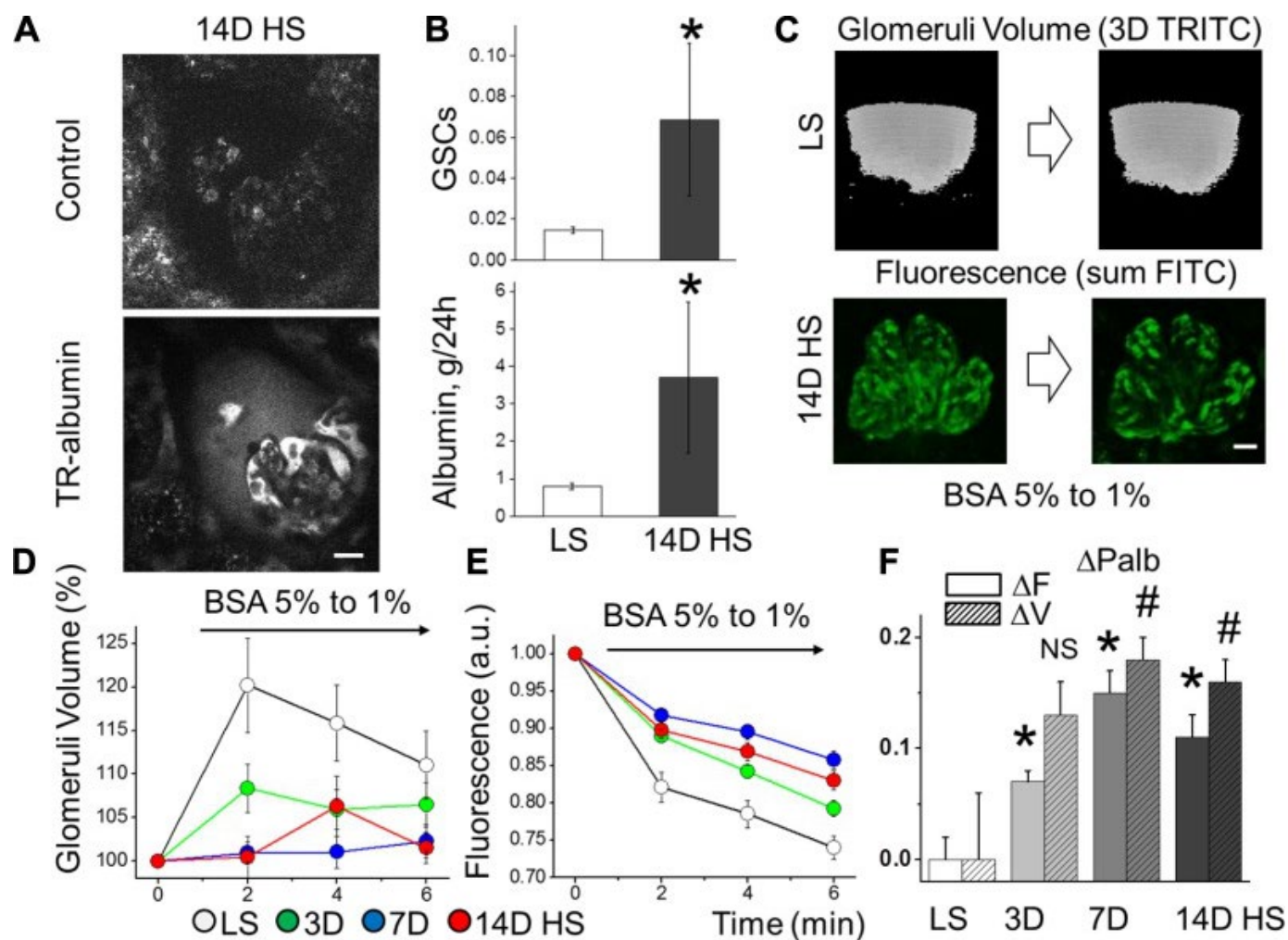
Hypertensive effects on glomerular sieving of albumin (GSC_{alb}) measured in vivo and glomerular permeability to albumin measured ex vivo. *A*: representative intravital images demonstrating glomerulus before and after infusion of Texas Red (TR)-labeled albumin. These images revealed a significant increase in albumin concentration in the Bowman's space of SS rats following consumption of a high-salt diet for 14 days (14D HS). Scale bar, 20 μm. *B*, *top*: GSC_{alb} assessed with intravital imaging in SS rats fed LS and HS (14 days) diets ($n \geq 5$ for each group; $*P < 0.05$). *B*, *bottom*: estimated amount of daily filtered albumin. *C*: glomeruli were extracted and glomerular permeability studies performed by exposing isolated glomeruli to oncotic gradients (changing BSA from 5 to 1% solution). Fluorescent intensities of FITC albumin and TRITC dextran were monitored by confocal laser scanning. A z-stack of 26 consecutive focal planes (73.83 μm) was collected every 2 min, which allowed for the monitoring of fluorescence within glomerular capillaries (FITC) and surrounding the glomerulus to measure glomerular volume (TRITC) in 3-dimensional reconstruction. *D*: changes in glomerular volume (% maximum volume change) in SS rats fed a LS vs. 3D, 7D, and 14D on HS; $n \geq 11$, $P < 0.05$. *E*: fluorescence created by the oncotic gradient following HS consumption ($n \geq 17$, $P < 0.05$). *F*: changes in permeability to albumin (ΔP_{alb}; $n = 11$ glomeruli/group) calculated from the volume (ΔV) measurements (hatched bars; $\#P < 0.05$ compared with LS) and fluorescent (ΔF) measurements (solid bars; $*P < 0.05$ compared with LS).
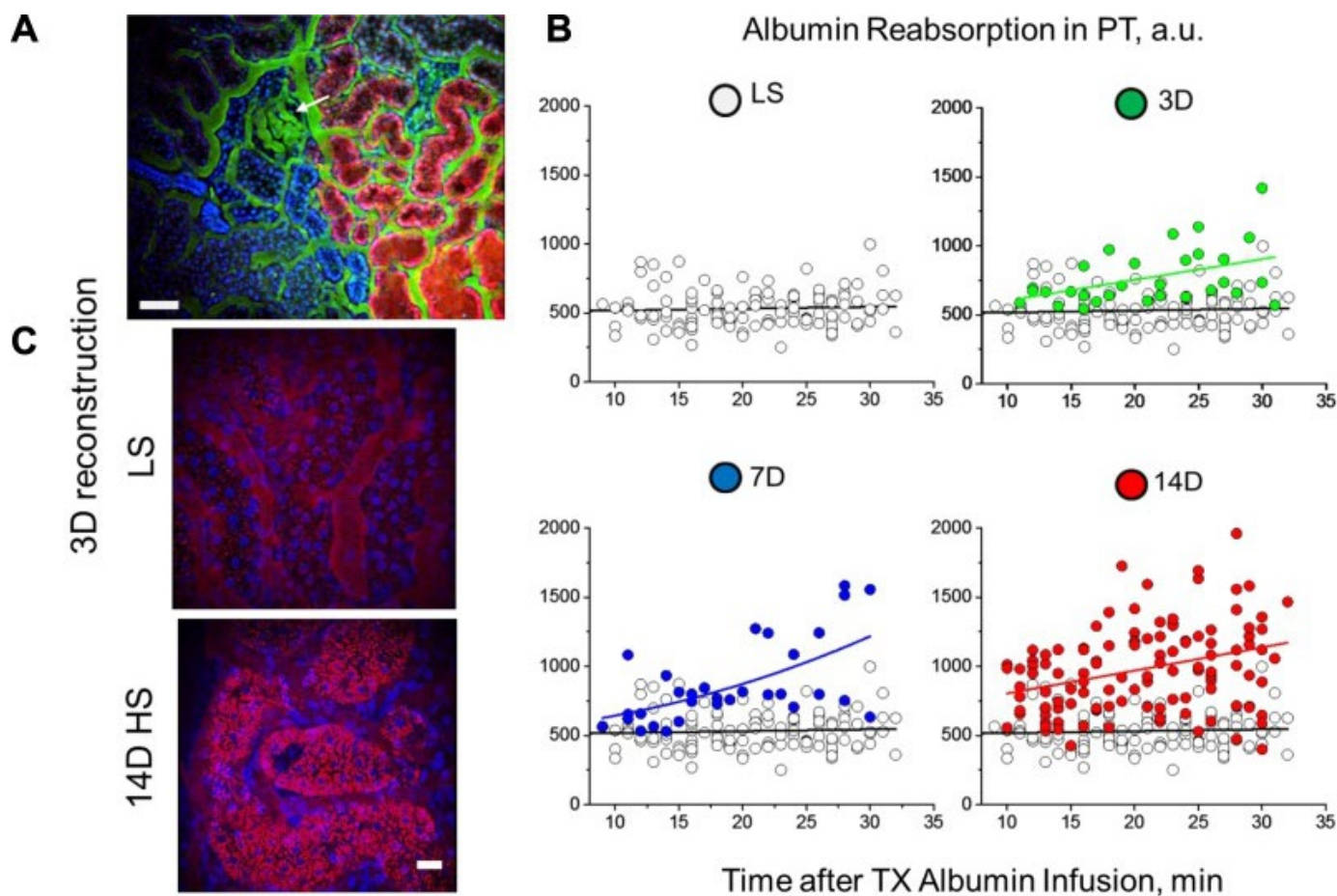
Fig. 3.

Evaluation of proximal tubular reabsorption of albumin during salt-sensitive hypertension. *A*: 3-dimensional reconstruction of low-magnification screening (IRAPO ×25 W objective, NA 1.0; Leica) shows the glomerulus (arrow), albumin filtered through and actively reabsorbed by proximal tubules (TR-albumin; red), vasculature (150-kDa FITC-labeled dextran; green), and nuclear staining (Hoechst; blue) in proximal and distal (dense blue color) tubules. Scale bar, 100 μm. *B*: time-dependent changes in TR-albumin (from the initial infusion to >30 min) in proximal tubule (PT) of SS rats fed a LS or HS (3D, 7D, and 14D) diet. Note that PT albumin reabsorption in rats fed a LS diet showed a linear dependence with well-balanced uptake and transcytosis (○). Control reabsorption values are plotted in all of the graphs to demonstrate the differences before and after HS treatment. PT reabsorption increased significantly in a stepwise manner under HS conditions (no. of tubules varies from 30 for 3D and 7D to 110 for LS and 14D groups). *C*: representative images of PT reabsorbing TR-albumin (28 min after infusion) following consumption of a LS or 14D HS diet (3-dimensional reconstruction of 25 z-stack intravital images). Note the significant increase in TR-albumin (red) reabsorbed by PT under HS diet conditions. Scale bar, 20 μm.

Fig. 4.
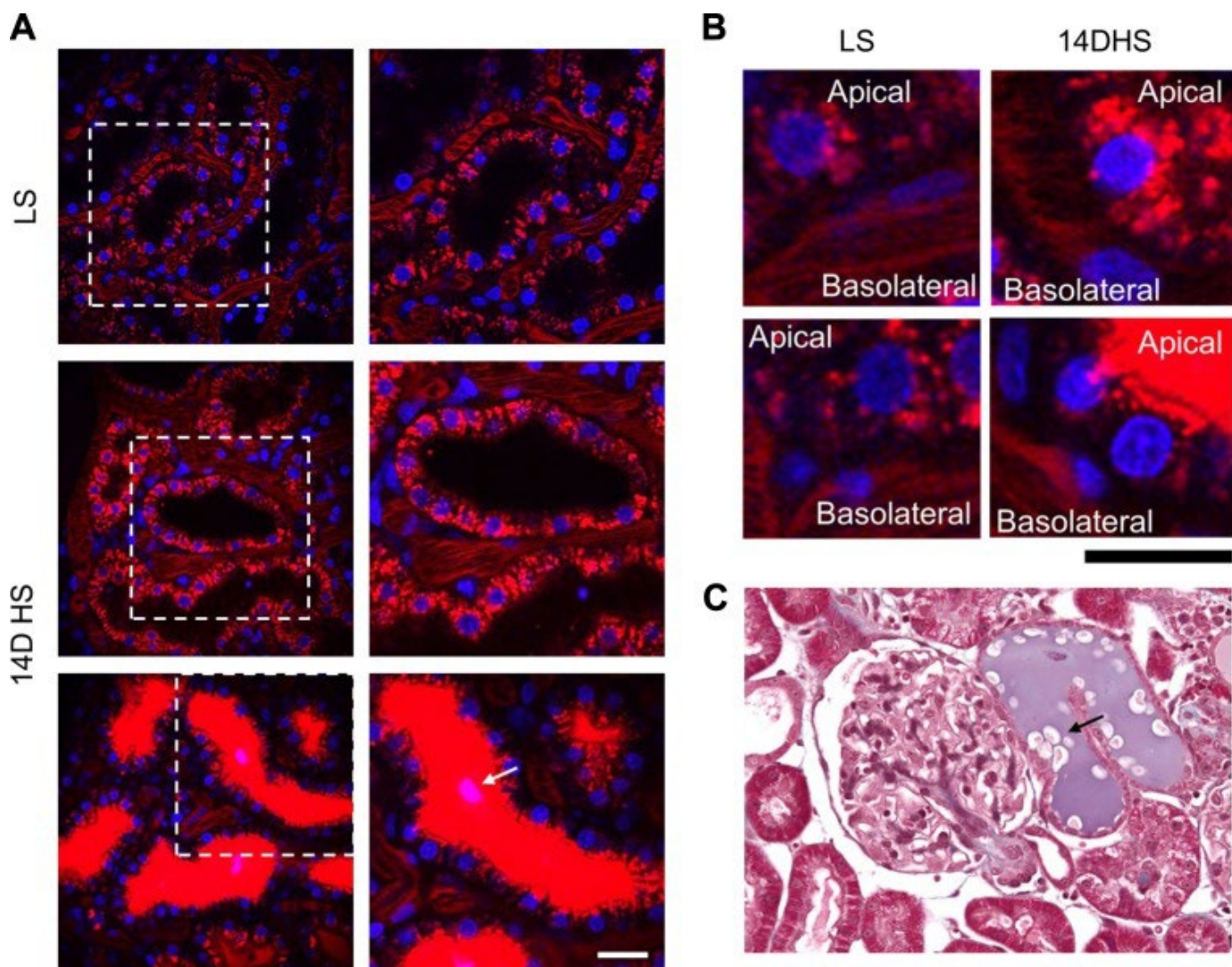
Reabsorption of albumin by proximal tubule cells and cell damage during salt-sensitive hypertension. *A*: intarvital imaging of PT after 25 min postinjection of TR-albumin (red) into blood circulation at LS and 14 days of HS. Note the significant accumulation of TR-albumin in PT in the case of substantial glomerular leakage of proteins (*bottom*). Scale bar, 20 µm. *B*: high-magnification images of PT and microvascular area under the conditions described in *A*. Scale bar, 10 µm. Note the high density and different localization of TR-albumin in PT cells at HS conditions. *C*: representative kidney section from SS rats fed HS diet. Arrow shows protein casts in both intravital (*A*) and immunohistochemical (*C*) images of PT.

Fig. 5.
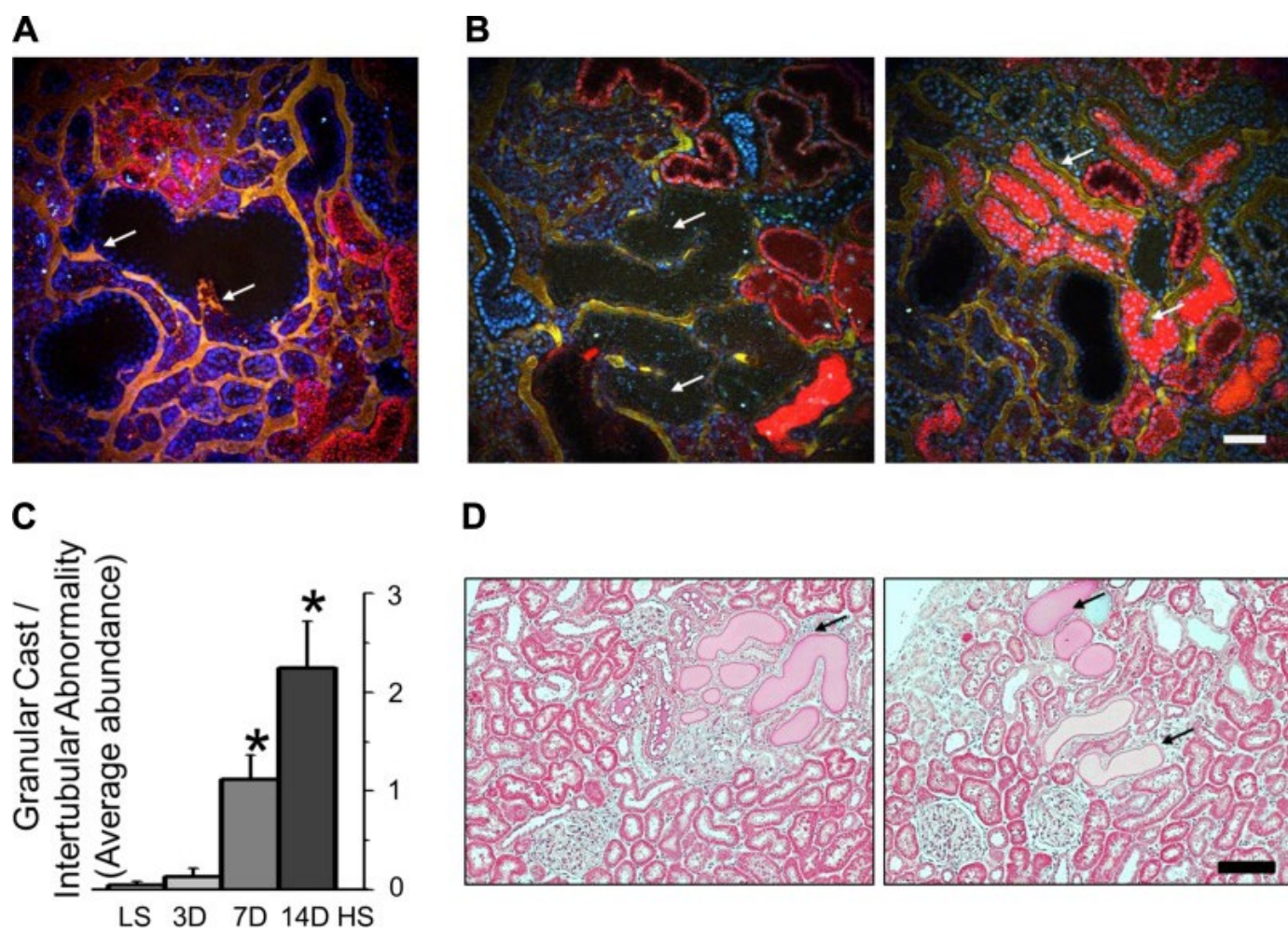
Proximal tubule (PT) damage during development of salt-sensitive hypertension and albuminuria. *A*: 3-dimensional reconstruction of the kidney section from an SS rat fed a HS for 14 days assessed with intravital imaging. Shown are dilated PT (wide black areas) and changes in perivascular beds (arrows; yellow color represents mix of red and green channels, TR-albumin, and 150-kDa FITC-labeled dextran correspondingly). *B*: low-magnification screening revealed large PT segments with dilated epithelium, granular cast material, and other intertubular abnormalities that resulted in the absence of albumin reabsorption or urine flow. Shown with arrows are cystic-dilated PT (*left*) and flooding with TR-albumin (*right*). *C*: summary graph of PT damage (score of 3 indicates the most severe injury; $n = 10$ rats/group, with ≤ 15 images analyzed for each rat; *$P < 0.05$). *D*: kidney sections from SS rats fed a HS diet for 14 days. Shown are protein casts and PT tubular damage (arrows). Scale bars, 100 μm for all images.

Fig. 6.
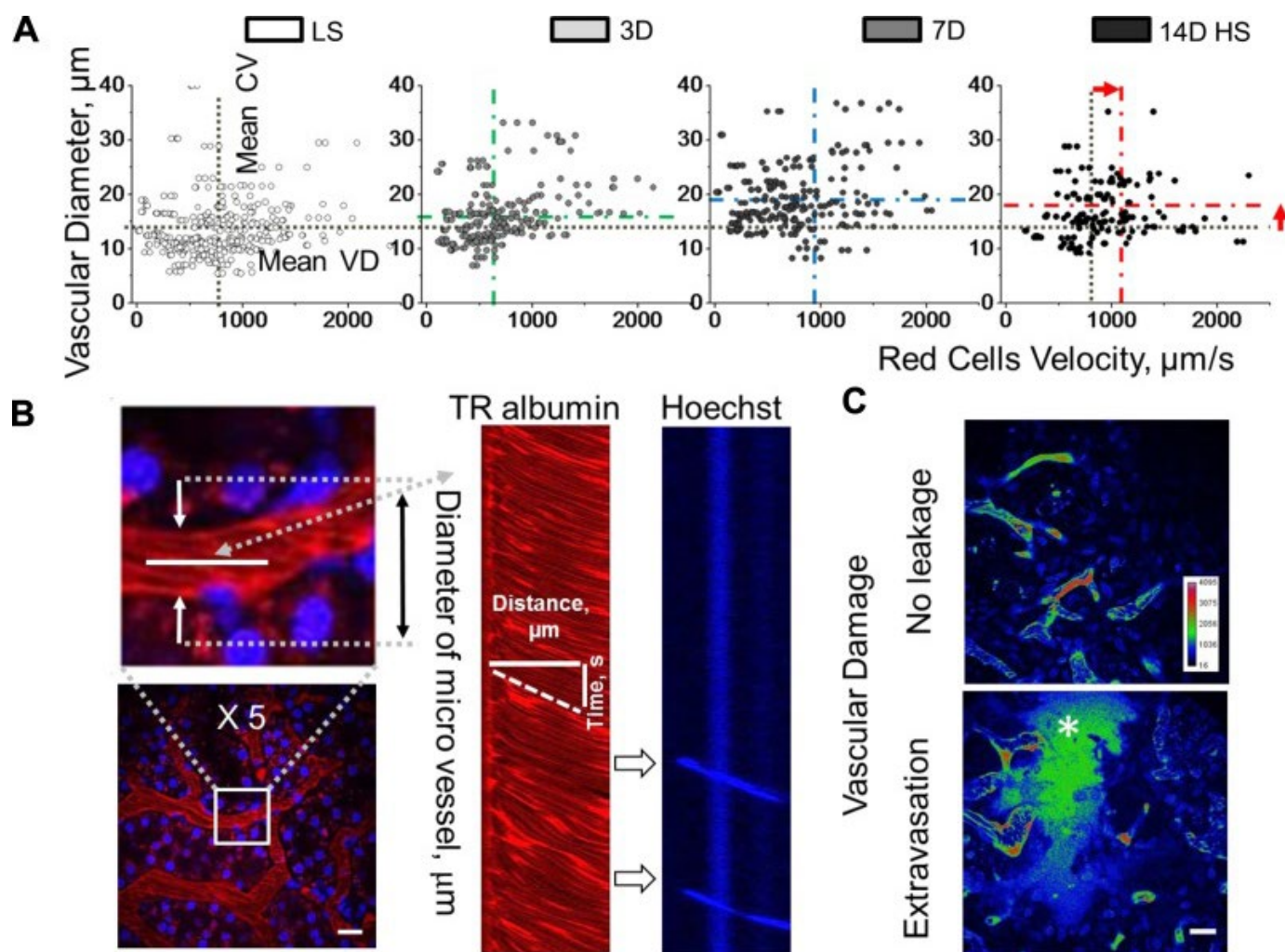
Assessing blood flow and vascular pathologies in the kidney. *A*: cortical renal blood vessel flow rates were evaluated by scanning red blood cell (RBC) velocity. Changes in blood flow and vascular diameter following high salt consumption; n = 339, 225, 225, and 225 vessels for LS, 3D, 7D, and 14D HS, respectively; *$P < 0.05$ for LS compared with 7D and 14D HS. *B*: representative images demonstrating the blood vessel line scans used to measure RBC velocity (μm/s) and microvessel diameter (μm). At *right* is a line scan example that tracks the movement of red blood (red) or white cells (blue) correspondingly. *C*: vascular extravasation of high-molecular weight molecules was assessed by injecting of 150-kDa FITC-Dextran and scoring the obtained indexed images in the renal cortex of experimental animals ($P < 0.05$). *Top* (LS-fed rats): there is no leakage of the 150-kDa Dextran into the interstitial space. *Inset*: shows the color intensity calibration bar. *Bottom* (14D HS-fed rats): high-intensity fluorescence within the interstitial space (*) closely matching the plasma intensity. Scale bars, 100 μm for all images.